Development of a lamp-pumped Cr:LiSAF laser operating at 20Hz for a terawatt CPA system

Ricardo E. Samad, Gesse E. C. Nogueira, Sonia L. Baldochi and Nilson D. Vieira Jr
IPEN/CNEN-SP – Centro de Lasers e Aplicações
Av. Prof. Lineu Prestes 2242, 05508-000, São Paulo, SP, Brazil

ABSTRACT

We report here the development, construction and characterization of a flashlamp pumped Cr:LiSAF rod pumping cavity designed to minimize the thermal load on the crystal. The cavity is a close coupled one with 2 Xe lamps and absorptive filters between the lamps and the Cr:LiSAF rod, and is refrigerated with cooled water. A compact and stable ($g_1 \cdot g_2$=0.57) resonator was designed for lasers tests and gain medium characterization, and we expected to obtain operation at 20 Hz repetition rate. Nevertheless, the thermal load minimizing design was so successful that allowed laser operation up to 30 Hz with an average power of 20 W. When operating with a 10% transmission output coupler this laser exhibited an overall laser efficiency of 0.6% under 100 J electrical pumping, and a slope efficiency of 0.8%. Under these conditions, a maximum gain per pass of 1.5 was obtained, suitable for regenerative amplifiers. To increase the gain, the intracavity filters were substituted by glass plates, resulting in a gain per pass of 3.6, adequate for multipass amplifiers. In this configuration, and operating as a laser resonator, it showed a maximum overall efficiency of 2.81% under 88 J electrical pumping with a 25% transmission output coupler, and maximum output power of 18 W at 8 Hz. A study of the thermal load on the crystal was conducted by observation of the upper laser level lifetime, and we concluded that there are no noticeable accumulated thermal effects on the Cr:LiSAF emission.

1. INTRODUCTION

Single crystals of Cr:LiSAF (Cr^{3+}:$LiSrAlF_6$) show very attractive optical spectroscopic properties[1] for a potential laser medium, such as a long lifetime of the upper laser level (~67μs) at room temperature[2], three broad absorption bands[2] and a wide emission band ranging from 650 nm to 1050 nm. Laser action was demonstrated under several pumping schemes[2, 3, 4, 5], particularly in CW[6] and pulsed regimes. Pulse durations ranging from hundreds of microseconds under free-running pulsed excitation down to nanoseconds in Q-Switching and few femtoseconds in Mode-Locking regime[7] were achieved.

Flashlamp-pumped Cr:LiSAF tunable lasers[3, 8, 9, 10] have been developed reaching pulse energies up to 8.8 J, and flashlamp pumped ultrashort pulse amplifiers[11, 12, 13, 10] reached peak powers up to 8.5 TW. Due to the poor thermal properties of the LiSAF host[14], the operation repetition rate of these lasers/amplifiers were always confined either to the single pulse regime or up to 12 Hz[8]. The low LISAF thermal conductivity leads to crystal cracking due to thermally induced stress, and in the case of a gain medium in the shape of a rod, fracture was observed at 18 Hz[15]. Besides the thermal induced stress that leads to fracture, the lifetime of the Cr:LiSAF laser transition is strongly temperature dependent, dropping from ~67 μs at room temperature to half this value at 69°C, due to thermal quenching[16]. Under flashlamp pumping, the low LiSAF thermal conductivity prevents heat extraction from the laser medium. If the crystal temperature rises above ~25°C, the nonradiactive decay generates more heat, what in turn increases the nonradiactive decay rate, rapidly increasing the crystal temperature. This is a catastrophic process that reduces the energy storage capacity of the crystal and can lead to fracture.

In order to avoid thermal quenching and crystal fracture due to accumulated heat, flashlamp pumped Cr:LiSAF oscillators have been kept operating at low repetition rates. Shimada et al.[8] reported the highest repetition rate and power on a Cr:LiSAF laser to be 4.5 W at 12 Hz, and Perry et al.[17] reported the highest amplifier repetition rate to be 10 Hz. Alternatively, a slab geometry laser[9] scheme requires small thickness of the gain medium, allowing for better heat extraction and therefore a lower stress in the gain medium and in this case the laser achieved pulse energies as high as 8.8 J, but at 5 Hz repetition rate.

Aiming to raise the repetition rate of flashlamp pumped Cr:LiSAF rod lasers and amplifiers, still keeping its gain and power, we propose a different approach that minimizes the crystal thermal load and temperature gradient by decreasing the heat reaching the gain medium and being generated inside it. To study this scheme, a flashlamp pumped Cr:LiSAF rod laser was developed and constructed. This scheme was developed aiming to obtain laser operation at 20

Laser Beam Control and Applications, edited by Alexis V. Kudryashov, Alan H. Paxton, Vladimir S. Ilchenko, Adolf Giesen, Detlef Nickel, Steven J. Davis, Michael C. Heaven, J. Thomas Schriempf,
Proc. of SPIE Vol. 6101, 610112, (2006) · 0277-786X/06/$15 · doi: 10.1117/12.644145

Hz repetition rate, but was so successful that the laser could be operated at repetition rates as high as 30 Hz, with an average power of 20 W, and a maximum gain of ~50% per pass. Modifying the pumping scheme higher gains up to 4 per pass were obtained, but at lower repetition rates.

2. PUMPING CAVITY CONCEPTION AND LASER DESIGN

We developed a flashlamp pumped pumping cavity, aiming to minimize the rod thermal load and to increase the laser repetition rate. The rod has a 1.5mol% Cr doping, 101.6 mm of length and 6.35 mm of diameter, with Brewster angled faces. Small diameters allow the extraction of heat more efficiently from the bulk of the rod, decreasing the temperature gradient that leads to rod fracture. The cavity has two 4″ arc-length, 7 mm bore, 450 torr Xenon flashlamps, each one independently fed by a power source capable of delivering up to 50 J in ~67 μs (FWHM) pulses. The power sources were triggered and synchronized by a Stanford Research Systems DG535 delay generator. The pulse width was chosen in order to match the laser transition lifetime, consequently decreasing heat generation by pump energy that is lost to spontaneous emission. The cavity is a closed coupled one, with an alumina diffuse reflector, and cooled by deionized water at 11°C and 30 psi in turbulent flow regime. The humidity in the laboratory is kept under 40%, lowering the dew point, avoiding water condensation on the rod surfaces.

The temperature of the laser medium inside a pumping cavity is determined by how much energy is absorbed by the medium, and the amount of that energy that is not converted into light emission (spontaneous or stimulated), and how this excess energy is extracted. The main heat source for the Cr:LiSAF crystal is the Stokes-Shift from the three absorption bands centered at 290 nm, 450 nm and 650 nm to the emission band at 830 nm. For a photon absorbed at the center of the 290 nm band resulting in an emitted photon at 830 nm, about 65% of its energy is converted into heat due to the Stokes-Shift. For photons absorbed at the center of the 430 nm and 650 nm bands, these fractions are 50% and 24%, respectively. With the purpose minimizing the heat in the rod, optical filters were inserted into the pumping cavity between the rod and each one of the flashlamps, absorbing all light below 600 nm and above 700 nm, as shown in Figure 1. In this way, only the 650 nm band is excited, decreasing the Stokes-shift generated heat to only ~25% of the absorbed power. Besides, the filters also block the infrared heat component radiating from the flashlamps. The pumping cavity was designed in a way that the optical filters divide it in three compartments, isolating the rod from the flashlamps, allowing independent coolant flow around each component. The cooling water flows around the rod, and then refrigerates the flashlamps. Thus, heat transfer from the flashlamps to the rod by the cooling water is avoided. In Figure 2 a scheme of the pumping cavity is shown.

The optical resonator was built using a 1 m curvature radius concave High-Reflector mirror located 21 cm away from one rod end, and a plane output coupler located 12 cm from the other end of the rod, resulting in a stability product[18] $g_1 \cdot g_2 = 0.57$ for an empty resonator. Plane output couplers with reflections ranging from 55% to 96% at 850 nm were used to characterize the laser performance.

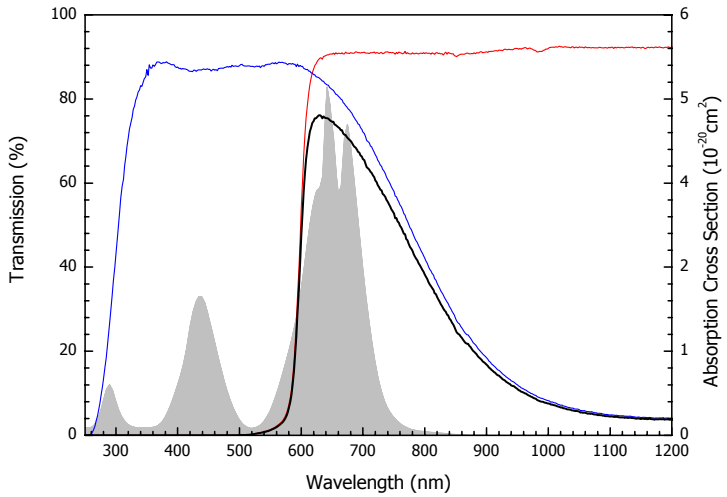

Figure 1 – Transmission spectra of the intracavity filters (thin lines, left scale). The thick line is their convolution, indicating the fraction of the flashlamps light that reaches the Cr:LiSAF rod. The shaded region is the Cr:LiSAF absorption cross section parallel to the c-axis (right scale).

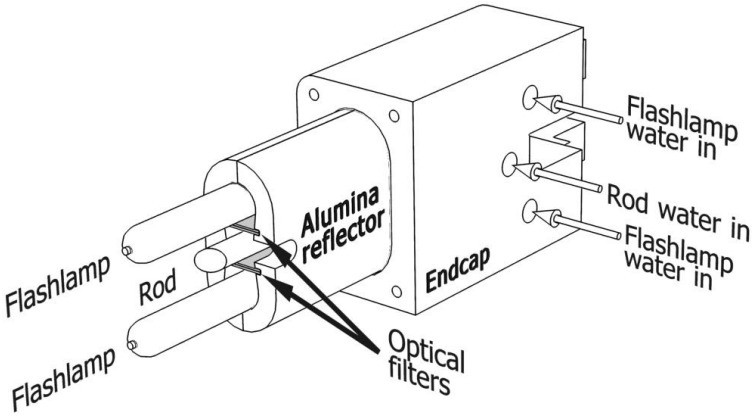

Figure 2 - Scheme of the pumping cavity without an endcap. The different cooling water entrances for cooling the crystal and flashlamps are indicated; the optical filters, located between each flashlamp and the crystal, divide the pumping cavity into three independent cooling chambers.

3. RESULTS

The complete characterization of the laser is reported elsewhere[19]. Here we describe only the results relevant to the pumping cavity operation as an amplifier.

The laser output pulse energy as a function of one of the flashlamps input energy, for eight different output coupler reflectivities (R_{OC}), is shown in Figure 3. The data for the highest reflectivity (R_{OC}=95.9%) output coupler is limited to energies under 14 J/flashlamp because the mirror was damaged at that pump energy due to absorption losses. In Table 1 we present the total (2 flashlamps) pump energy threshold for laser action for each output coupler and the corresponding slope efficiencies. The maximum total measured efficiency is 0.65% for R_{OC}=89.3% at 100 J pumping energy.

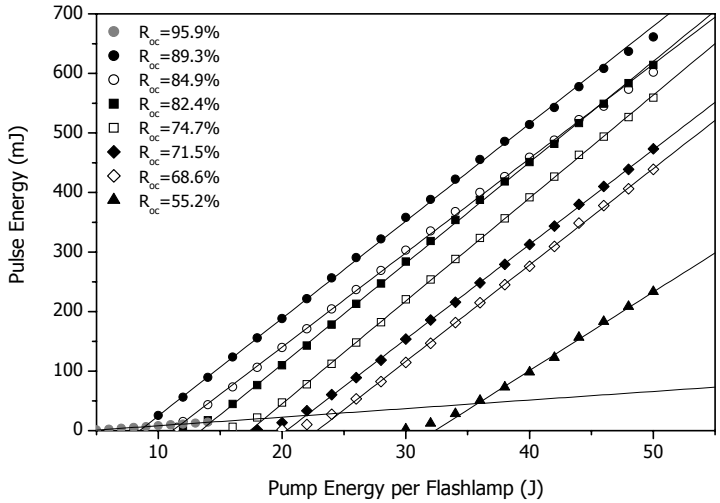

Figure 3 - Cr:LiSAF laser slope efficiencies for various output couplers reflectivities (R_{OC}) along with linear fitted functions for each output coupler, as a function of the pump energy per flashlamp. For each R_{OC} data set, the two or three lower energy points were disregarded in the fitting due to the unstable laser oscillation near the threshold.

Table 1. Values obtained from the fitted functions shown in Figure 3, for each output coupler

R_{OC} (%)	$-\ln(R_{OC})$	E_{th} (J)	Slope Eff. (%)	$g_t\ell$	*Gain per pass*
95.9 ± 1.0	0.042 ± 0.010	8.68 ± 0.28	0.072 ± 0.001	0.045 ± 0.006	1.046 ± 0.006
89.3 ± 0.4	0.113 ± 0.004	16.96 ± 0.24	0.818 ± 0.004	0.081 ± 0.005	1.084 ± 0.005
84.9 ± 0.6	0.164 ± 0.007	22.28 ± 0.22	0.792 ± 0.004	0.106 ± 0.006	1.112 ± 0.007
82.4 ± 0.5	0.193 ± 0.006	26.86 ± 0.22	0.848 ± 0.003	0.121 ± 0.005	1.129 ± 0.006
74.7 ± 0.6	0.292 ± 0.008	34.80 ± 0.24	0.865 ± 0.003	0.170 ± 0.006	1.185 ± 0.007
71.5 ± 0.5	0.335 ± 0.007	40.68 ± 0.34	0.799 ± 0.004	0.192 ± 0.006	1.212 ± 0.007
68.6 ± 0.5	0.377 ± 0.007	45.64 ± 0.46	0.810 ± 0.005	0.212 ± 0.006	1.236 ± 0.007
55.2 ± 0.5	0.594 ± 0.009	64.7 ± 2.0	0.66 ± 0.01	0.321 ± 0.006	1.379 ± 0.008

From the data in the second and third columns in Table 1 the resonator losses were determined through a Findlay-Clay analysis[20]. This analysis consists of fitting a line to the data of $-\ln(R_{OC})$ as a function of the lasing threshold pump energy, and the resonator losses are given by the point where the line crosses the y-axis. The data fitted by the line is shown in Figure 4, resulting in total resonator losses L with value L=(4.8 ± 0.9) %. It is then possible to calculate the threshold gain, given by[18]:

$$g_t \ell = \tfrac{1}{2}\left[L - \ln(R_{OC})\right] \qquad (1)$$

where g_t is the threshold small-signal gain and ℓ is the rod length. From equation (1) the threshold gain can be determined for each output coupler and its values are shown in the fifth column of Table 1, along with the threshold gain per pass in the sixth column.

In Figure 5 we plot the calculated gain per pass as a function of the measured threshold pump energy (Table 1) along with a fitted linear function. The extrapolation of this function gives a gain per pass of (1.54±0.03) at 100 J of pumping energy.

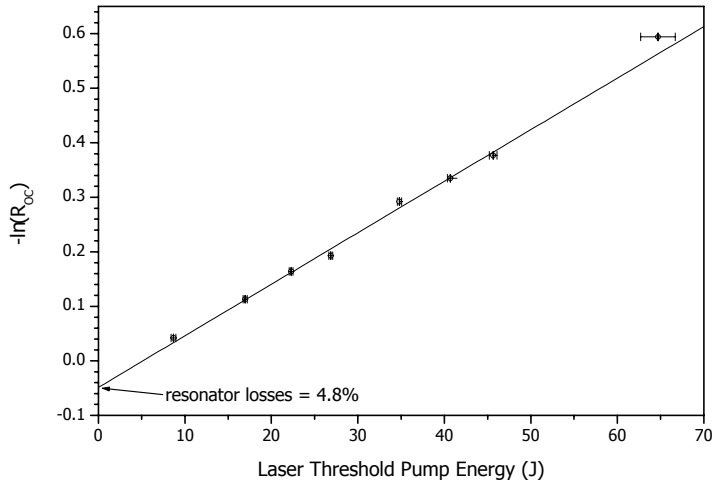

Figure 4 – Findlay-Clay analysis of the Laser. The fitted line crosses the y-axis at -0.048, providing the resonator losses.

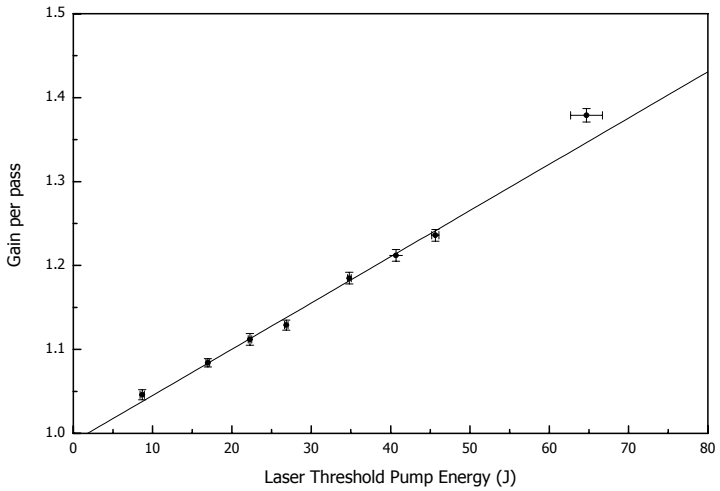

Figure 5 – Gain per pass as a function of the threshold pump energy and fitted line.

Figure 6 shows the pulse energy dependence on the pump repetition rate. It can be seen that for 60 J pumping level, the pulse energy is almost constant, varying about 3% around its average value. For higher pump energies, a decrease of the pulse energy with increasing repetition rate is observed. At 100 J and 30 Hz, this pulse energy drop is 8% of its value at 1 Hz. The maximum measured pulse energy at 30 Hz is (660.4±9.4) mJ, resulting in an average power of 19.8 W.

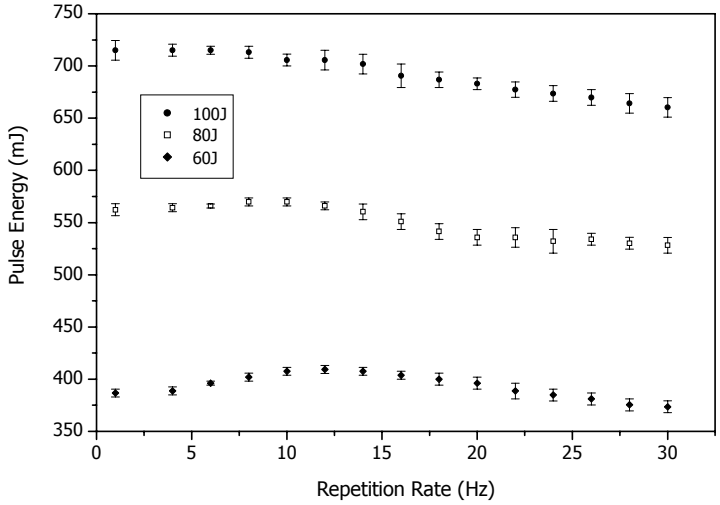

Figure 6 - Dependence of the pulse energy on the pump repetition rate for different pumping energies. The output coupler reflectivity is R_{OC}=89.3%.

To investigate if the energy dropping at higher repetition rates is due to the lifetime shortening as a consequence of rod heating and thermal quenching, the temporal shapes of the flashlamp pulse and of the spontaneous emission were simultaneously measured with fast detectors and an averaging oscilloscope (Lecroy WaveRunner 6051) for various repetition rates, at the higher pump energy (100 J). An empirical function was fitted to the flashlamps emission temporal shape, and this fitted function was used as the pumping term $I_p(t)$ to numerically solve the population rate equation for the Cr:LiSAF system:

$$\frac{dN_2}{dt} = N_0 I_P(t) - \frac{N_2}{\tau} \qquad (2)$$

where N_0 and N_2 are the Cr^{3+} ground and excited state populations, respectively, and the spontaneous emission follows the excited state population $N_2(t)$. The lifetime of the excited state, τ, was considered as an adjustable parameter and was tuned to obtain the best agreement between the acquired data for the spontaneous emission and the $N_2(t)$ curve resulting from equation (2) numerical integration. This procedure was performed for 100 J pumping and repetition rates ranging from 2 Hz to 30 Hz. For all repetition rates, the best agreement between the experimental and numerical Cr:LiSAF spontaneous emission curves always occurs for τ=64 μs although the flashlamp pulse duration increases almost 5% from 4 Hz to 30 Hz. In Figure 7, the measured flashlamps emission and rod spontaneous emission temporal profiles are presented together with the flashlamp temporal fit and the emission numeric solution for 4 Hz and 30 Hz repetition rates. The criteria for checking the agreement between data and numerical solution was the emission peak position. The spontaneous emission decay was not chosen because the fitted function to the flashlamps emission drops slower than the measured data and consequently causes a slower spontaneous emission decay. The fact that the same lifetime (64 μs) provided the best agreement for all repetition rates from 2 Hz to 30 Hz indicates that there is no quenching of the luminescence due to increased thermal load in the crystal as the repetition rate grows. The energy drop shown in Figure 6 is probably due to slight changes in the flashlamps and in the power sources behavior and efficiency, as the repetition rate increases. Although the absolute value obtained for the Cr:LiSAF lifetime differs from the accepted one[2] of (67 ± 5) μs, it is within its precision measurement. Nevertheless, the value agrees with the one measured[16] at 77 K that is predicted to be the same at room temperature.

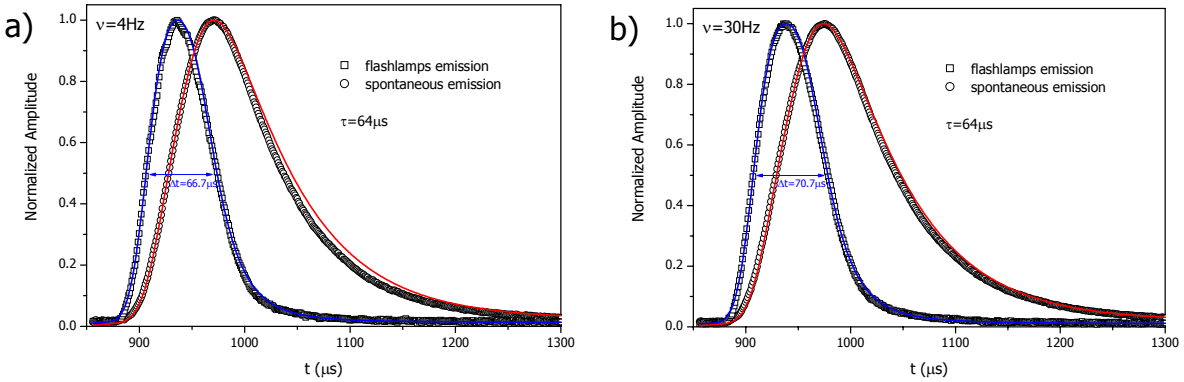

Figure 7– experimental measured flashlamps emission at 100 J (open squares) and Cr:LiSAF spontaneous emission (open circles), with the empirical function fitted to the flashlamps emission and the numerical solution of the Cr:LiSAF rate equation for τ=64 μs (solid lines), normalized to (peak amplitude)=1. In the curves for a) 4 Hz and b) 30 Hz, the flashlamp pulse duration (FWHM) is indicated. The time axis starts at 850 μs due to the relative delay between the trigger and the detectors signals.

The gain calculated at 100 J pumping, with value (1.54±0.03) is suitable for a regenerative amplifier[18], but is small for a multipass amplifier in which single pass gains over 3 are expected. In order to increase the gain, we opted to substitute the intracavity filters by glass plates. Glass has a cutoff around 300 nm, blocking the UV spectrum. With these plates, the 650 nm and 450 nm bands are pumped along with the lower energy wing of the 290 nm band, what is expected to increase the gain at the cost of a greater thermal load in the rod. For this configuration, in Figure 8 the measured values of the laser pulse energy are plotted as a function of the pumping energy for the same output couplers of Figure 3 (except for the R_{OC}=95.9% mirror that was damaged). The maximum pulse energy measured was (2.80±0.1) J at 100 J pumping with the R_{OC}=74.7% mirror, and the maximum total efficiency measured was 2.81% at 88 J pumping with the R_{OC}=82.4% mirror. The higher average power measured was 18 W at 8 Hz for the R_{OC}=74.7% mirror, at 100 J pumping. Following the same procedure as before, in Table 2 we present the threshold pump energies, slope efficiencies, threshold small signal gain and gain per pass for each one of the output couplers in this new configuration with glass substituting the intracavity filters. The cavity losses, resulting from the Findlay-Clay analysis shown on Figure 9 are (16.4±2.9)%. In Figure 10 the measured gain per pass is shown as a function of the pumping energy along with a fitted linear function. Using this function to extrapolate the gain per pass to 100 J pumping results in a value of 3.33, adequate to a multipass amplifier. Direct measurement of the amplification of a 20 ps, 650 μJ pulse centered at 830 nm gave a gain per pass of 3.61. The discrepancy between the theoretical (3.33) and experimental (3.61) values obtained for the gain can be credited to the energy values used in the fit shown in Figure 10. The energies are restricted to below 20 J, so the

extrapolation of the fit to 100 J carries uncertainties. Nevertheless, the agreement between the inferred value and the measured one for the gain is quite good (they differ by less than 10%).

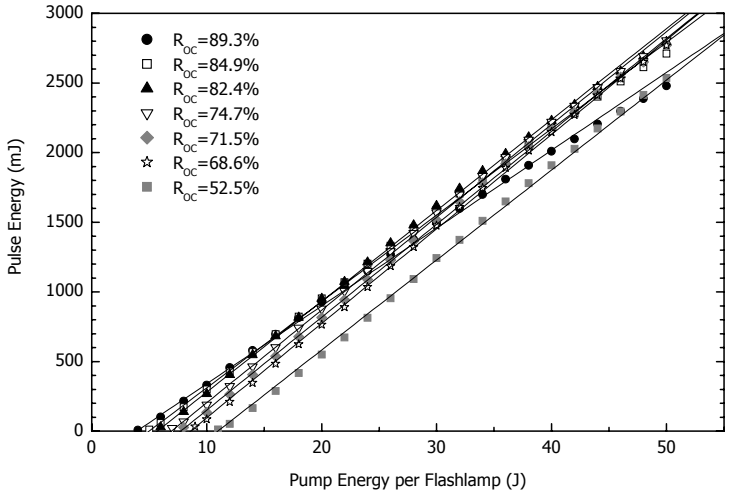

Figure 8 – Cr:LiSAF laser slope efficiency data for the cavity with glass plates substituting the intracavity filters.

Table 2. Values obtained from the fitted functions shown in Figure 8, for each output coupler

R_{OC} (%)	-ln(R_{OC})	E_{th} (J)	Slope Eff. (%)	$g_{t\ell}$	*Gain per pass*
89.3 ± 0.4	0.113 ± 0.004	7.84 ± 0.34	2.79 ± 0.02	0.138 ± 0.088	1.15 ± 0.10
84.9 ± 0.6	0.164 ± 0.007	9.96 ± 0.28	3.10 ± 0.02	0.164 ± 0.088	1.18 ± 0.10
82.4 ± 0.5	0.193 ± 0.006	11.36 ± 0.26	3.26 ± 0.02	0.178 ± 0.088	1.20 ± 0.11
74.7 ± 0.6	0.292 ± 0.008	13.86 ± 0.22	3.33 ± 0.02	0.228 ± 0.088	1.26 ± 0.11
71.5 ± 0.5	0.335 ± 0.007	15.46 ± 0.24	3.34 ± 0.02	0.250 ± 0.088	1.28 ± 0.11
68.6 ± 0.5	0.377 ± 0.007	17.20 ± 0.22	3.39 ± 0.02	0.270 ± 0.088	1.31 ± 0.12
55.2 ± 0.5	0.594 ± 0.009	21.92 ± 0.38	3.23 ± 0.02	0.379 ± 0.089	1.46 ± 0.13

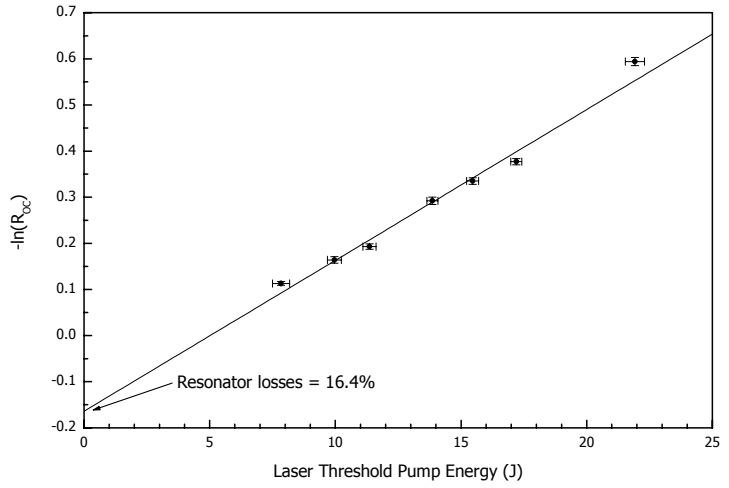

Figure 9– Findlay-Clay analysis of the Laser with the intracavity filters substituted by glass plates.

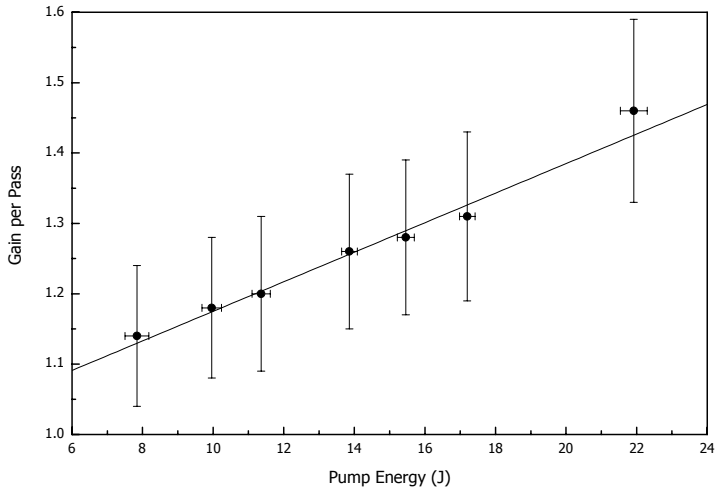

Figure 10 - Gain per pass as a function of the threshold pump energy and fitted line.

In Figure 11 we present the laser pulse energy dependence on the pumping repetition rate, up to 8 Hz. It can be seen that the pulse energy is constant for pumping energies up to 40 J. For higher pumping energies there is an output energy dropping as the repetition rate increases. At the higher pumping energy (100 J), this dropping at 8 Hz is almost 20% of the value at 1 Hz. To check if this dropping is due to increased thermal load at greater repetition rates, we proceeded as before and simultaneously measured the lamps emission and rod spontaneous emission at various pumping energies and repetition rates and numerically solved the rate equations. The results are shown in Figure 12, and it can be seen that, at a fixed pump energy, increasing the repetition rate does not change substantially the upper laser level lifetime, although this lifetime strongly depends on the pumping energy, what is clearly shown in Figure 13. This demonstrates that the energy decrease observed with the repetition rate increase is not due to luminescence quenching resulting from increased thermal load, and probably arises from the manifestation of a thermal lens that modifies the laser resonator. Also, we observe that the lifetime decreases as the pumping energy increases, most certainly as a result of local heating due to the Stokes shift, which is instantaneous. This heat is being removed by the cooling system, avoiding heat accumulation between pulses.

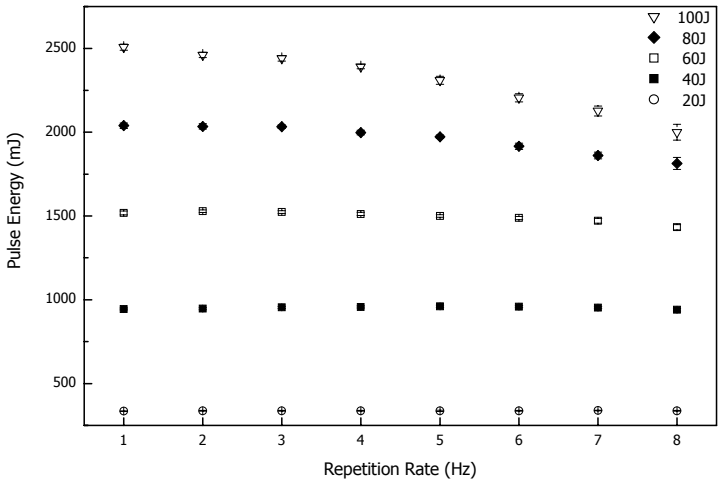

Figure 11 - Dependence of the pulse energy on the pump repetition rate for different pumping energies, with the intracavity filters substituted by glass plates. The output coupler reflectivity is R_{OC}=89.3%.

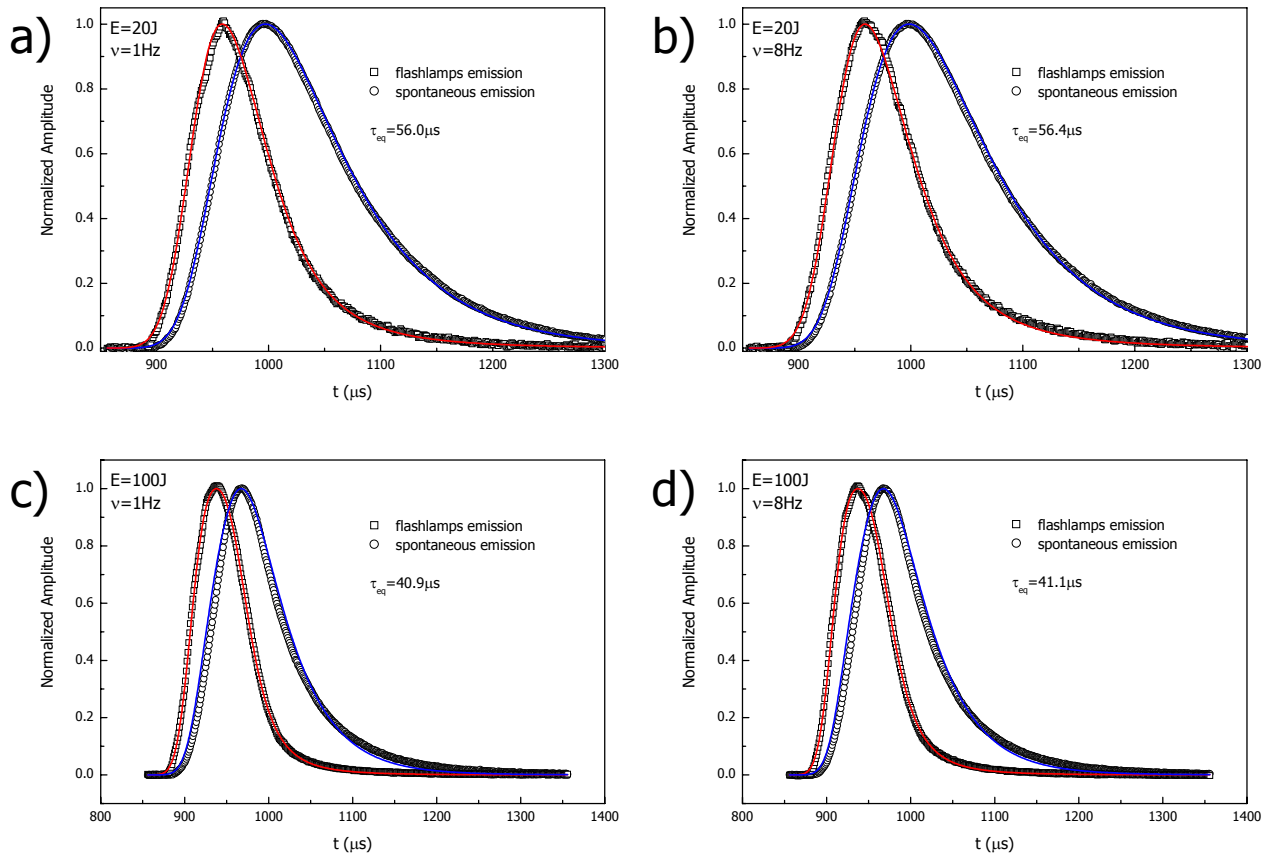

Figure 12 - experimental measured flashlamps emission (open squares) and Cr:LiSAF spontaneous emission (open circles), with the empirical function fitted to the flashlamps emission and the numerical solution of the Cr:LiSAF rate equation, all normalized to (peak amplitude)=1. In each graph the lifetime that provided the best agreement between the measured and numerically solved spontaneous emissions is indicated. a) 20 J pumping and 1 Hz repetition rate; b) 20 J pumping and 8 Hz repetition rate; c) 100 J pumping and 1 Hz repetition rate; d) 100 J pumping and 8 Hz repetition rate.

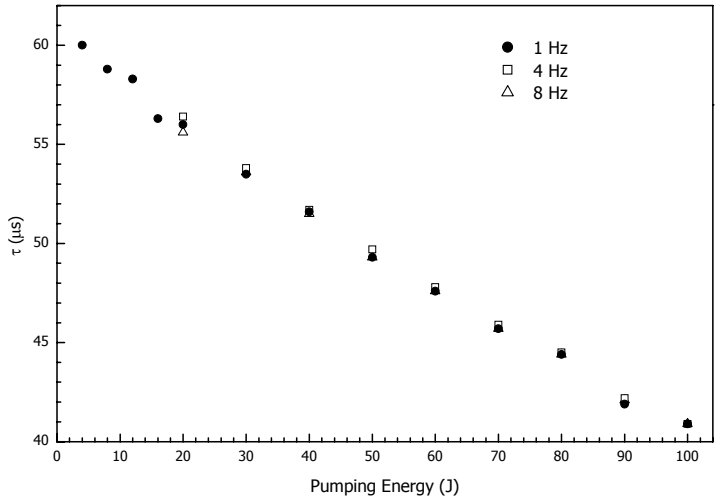

Figure 13 – Upper laser level transition lifetime that provides the best agreement between the measured spontaneous emission and the numerical solution of the rate equation, as a function of the pumping energy, for three repetition rates.

4. CONCLUSIONS

We developed a flashlamp pumped Cr:LiSAF pumping cavity with intracavity filters that reduced the thermal load in the crystal rod, so, in spite of the LiSAF low thermal conductivity, the laser repetition rate could be increased. The laser could be operated up to 30 Hz with an average power of 20 W, well above the reported values at which the rod is damaged. The resonator losses (4.8% per pass) and gain dependence on the pumping were calculated. Although the efficiency was reduced by the insertion of filters that prevented the pumping of the higher energies absorption bands, a maximum gain per pass over 1.5 was inferred, suitable for regenerative amplifiers for ultrashort pulses. No noticeable decrease in the lifetime of the laser transition was observed in the range of repetition rates and energies used, implying that our design could avoid significant laser rod temperature rise at high repetition rates. This indicates that the pumping cavity can be operated at even higher repetition rates and higher powers in lasers or amplifiers.

The substitution of the intracavity filters by glass plates that allow pumping in the 430 nm absorption band and also on the higher energy absorption band wing, increases the gain per pass to a measured value of 3.6 at the maximum pumping energy. This gain is suitable to ultrashort pulses multipass amplifiers. In this configuration a decrease of the laser pulse energy was observed with increased repetition rate, but we provided evidence that this is probably due to a thermal lens effect since no reduction of the life time is observed. A decrease of the lifetime was observed with increasing pump energy, evidencing that the Stokes-Shift generates heat instantaneously which in turn decreases the upper laser level lifetime. Even then, 18 W of average output power were obtained at 8 Hz and 100 J pumping.

We expected that, substituting the glass plates by filters that completely cut the 290 nm band, the gain should be slightly reduced, while the thermal effects (thermal lens and lifetime decrease due to Stokes-Shift) should be significantly reduced, once the 290 nm absorption band is small but more than 65% of its absorbed energy is converted into heat. This would allow operation at high gains and repetition rates.

ACKNOWLEDGMENTS

The Authors thank Dr. Wagner de Rossi for helpful discussions when designing the pumping cavity and the Fundação de Amparo à Pesquisa do Estado de São Paulo (FAPESP) for financial support under the grant 00/15135-9.

REFERENCES

1) Payne S. A., Chase L. L. and Wilke G. D., "Optical Spectroscopy of the New Laser Materials, $LiSrAlF_6$-Cr^{3+} and $LiCaAlF_6$-Cr^{3+}", *J. of Luminescence* **44**, 167-176 (1989).

2) S. A. Payne, L. L. Chase, L. K. Smith, W. L. Kway and H. W. Newkirk, "Laser Performance of $LiSrAlF_6$:Cr^{3+}", J. *Appl. Phys.* **66**, 1051-1065 (1989).

3) M. Stalder, B. H. T. Chai and M. Bass, "Flashlamp pumped Cr:$LiSrAlF_6$ laser", *Appl. Phys. Lett.* **58**, 216-218 (1991).

4) R. Scheps, J. F. Myers, H. B. Serreze, A. Rosenberg, R. C. Morris and M. Long, "Diode-pumped Cr:$LiSrAlF_6$ laser", *Opt. Lett.* **16**, 820-822 (1991)

5) B. Agate B, A. J. Kemp, C. T. A. Brown and W. Sibbett, "Efficient, high repletion-rate femtosecond blue source using a compact Cr:LiSAF laser", *Opt. Express.* **10**, 824-831 (2002).

6) M. Ihara, M. Tsunekane, N. Taguchi And H. Inaba, "Widely tunable, single-longitudinal-mode, diode pumped CW Cr:LiSAF laser", *Electron Lett.* **31**, 888–889 (1995).

7) S. Uemura and K. Torizuka, "Generation of 12-fs pulses from a diode-pumped Kerr-lens mode-locked Cr:LiSAF laser", *Opt. Lett.* **24**, 780-782 (1999).

8) T. Shimada, J. W. Early, and N. J. Cockroft, "Repetitively pulsed Cr:LiSAF for LIDAR applications", in *OSA Proc. Advanced Solid State Lasers*, 1994, pp. 188–191.

9) D. E. Klimek and A. Mandl, "Power Scaling of a Flashlamp-Pumped Cr:LiSAF Thin-Slab Zig-Zag Laser", IEEE *J. Quantum Elec.* **38**, 1607-1613 (2002).

10) H. Takada, K. Miyazaki and K. Torizuka, "Flashlamp-Pumped Cr:LiSAF Laser Amplifier", *IEEE J. Quantum Elec.* **33**, 2282-2285 (1997)

11) W E. White, J. R. Hunter, L. Van Woerkom, T. Ditmire, and M. D. Perry, "120-fs terawatt Ti:$A1_20_3$/Cr:$LiSrAlF_6$ laser system", *Opt. Lett.* **17**, 1067-1069 (1992).

12) Paul Beaud, Martin Richardson, Edward J. Miesak, and Bruce H. T. Chai, "8-TW 90-fs Cr:LiSAF laser", *Opt. Lett.* **18**, 1550-1552 (1993).

13) T. Ditmire, H. Nguyen, and M. D. Perry, "Amplification of femtosecond pulses to 1 J in Cr:$LiSrAlF_6$", *Opt. Lett.* **20**, 1142-1144 (1995).

14) S. A. Payne, L. K. Smith, R. J. Beach, B. H. T. Chai, J. H. Tassano, L. D. DeLoach, W. L. Kway, R. W. Solarz, and W. F. Krupke, "Properties of Cr:$LiSrAIF_6$ crystals for laser operation", *Appl. Opt.* **33**, 5526-5536 (1994).

15) F. Hanson, C. Bendall and P. Poirier, "Gain measurements and average power capabilities of Cr^{3+}:$LiSrAlF_6$", *Opt. Lett.* **18**, 1423-1425 (1993).

16) M. Stalder, M. Bass, and B. H. T. Chai, "Thermal quenching of fluorescence in chromium-doped fluoride laser crystals", *J. Opt. Soc. Am. B* **9**, 2271-2273 (1992).

17) M. D. Perry, D. Strickland, T. Ditmire and F G. Patterson, "Cr:$LiSrAlF_6$ regenerative amplifier", *Opt. Lett.* **17**, 604-606 (1992).

18) W. Koechner, Solid-State Laser Engineering (Springer Verlag, Berlin, 1999)

19) R. E. Samad, G. E. C. Nogueira, S. L. Baldochi and N. D. Vieira Jr., "Development of a flashlamp-pumped Cr:LiSAF laser operating at 30 Hz", accepted for publication in Applied Optics.

20) D. Findlay and R. A. Clay, "Measurement of internal losses in 4-level lasers", Phys. Lett. 20, 277-278 (1966).